IEEE Access
Multidisciplinary | Rapid Review | Open Access Journal

Received 15 May 2023, accepted 31 May 2023, date of publication 5 June 2023, date of current version 9 June 2023.

Digital Object Identifier 10.1109/ACCESS.2023.3283033

RESEARCH ARTICLE

Crop Response to Disease and Water Scarcity Quantified by Normalized Difference Latent Heat Index

MAI SON LE[1], YUEI-AN LIOU[2], (Senior Member, IEEE), AND MINH TUAN PHAM[1]

[1]Space Technology Institute, Vietnam Academy of Science and Technology, Cau Giay, Hanoi 10000, Vietnam

[2]Hydrology Remote Sensing Laboratory, Center for Space and Remote Sensing Research, National Central University (NCU), Zhongli, Taoyuan 320317, Taiwan

Corresponding author: Yuei-An Liou (yueian@csrsr.ncu.edu.tw)

This research was funded by Vingroup JSC and supported by the Postdoctoral Scholarship Programme of Vingroup Innovation Foundation (VINIF), Vingroup Big Data Institute (VinBigdata), code VINIF.2021.STS.29, and National Science and Technology Council, Taiwan.

ABSTRACT Early detection and quantification of plants' response to disease and water shortage conditions are very important for the agricultural management. This study represents the first utilization of Normalized Difference Latent Heat Index (NDLI) as a dimensionless indicator to assess plant health. By integrating NDLI with thermal infrared and surface energy balance (SEB) components, we aim to enhance the analysis of crop conditions and water scarcity in rice-growing areas. The integration between NDLI and land surface temperature exhibits a strong correlation ($r = -0.82$) with crop evapotranspiration (ET) derived from the widely used residual Surface Energy Balance Algorithm for Land model. Besides, the performance of NDLI- and SEB-based ET method proved its ability to provide the precise information of paddy field conditions by showing the significant correlations with the crop canopy biophysical properties that are traditionally represented and inferred by the multispectral remote sensing indices. The correlation coefficients of NDLI- and SEB-derived ET with Normalized Difference Vegetation Index (NDVI), Normalize Difference Water Index (NDWI), and Optimization of the Soil Adjusted Vegetation Index (OSAVI) were 0.84, 0.55, and 0.84, respectively. Also, NDLI- and SEB-derived ET exhibits a high degree of consistency with the ET determined through the SEBAL method, with difference less than 10% of the observations over 98.1% of the paddy fields of concern. Interestingly, the abnormally low ET signatures over the confirmed disease-infected regions of paddy fields are obviously observed in the NDLI- and SEB-derived ET maps, but not in the SEBAL-derived ET map. The findings of this work suggest that NDLI can be considered as a valuable indicator to provide information of the water stress status and health of the crop plants for advanced food-supply management.

INDEX TERMS Normalized difference latent heat index (NDLI), land surface temperature (LST), evapotranspiration (ET), surface energy balance (SEB).

I. INTRODUCTION

Detection of the plant's response to unfavourable conditions is an asset for timely and appropriate intervention for the targeting agricultural production [1]. Generally, the impairment of rice plant normal state can be directly or indirectly realized by a visual way [2]. However, such visual diagnosis is very much limited with scale, and ineffective and impractical for large-scale fields. Evapotranspiration (ET), known as one main component of the crop water requirements, represents the amount of water loss to the atmosphere during the process of plant growth and development [3]. Rapid determination of ET can be used for supplying accurate and timely information of crop water status to take suitable actions for production management [4].

Multispectral remote sensing provides great advancement for determining the land surface characteristics from micro to macro scales. Accordingly, various spectral indices have

The associate editor coordinating the review of this manuscript and approving it for publication was Gerardo Di Martino.

been successfully created and applied for the investigation of surface properties. The Normalized Difference Vegetation Index (NDVI) is widely used as a vegetation indicator [5] and it is associated with transpiration. The Normalized Difference Water Index (NDWI) was proposed to delineate the open water features [6] as the main source of evaporation. The Optimization of the Soil Adjusted Vegetation Index (OSAVI) is known as the optimization of the Soil Adjusted Vegetation Index, which was proposed to describe the dynamic soil-vegetation systems [7]. The spectral indices mentioned above play a crucial role as indicators, specifically designed to extract specific information from different land surface types. One such index, the Normalized Difference Latent heat Index (NDLI), has been proposed and proven to be a highly effective indicator for analyzing surface water availability characteristics based on spectral reflectance in the visible and near-infrared regions [8].

Furthermore, modelling algorithms have been proposed and applied for ET calculation. They can be segregated into three main categories: Simplified Empirical Regression [9], [10]; Surface Temperature – Vegetation Index Triangle/trapezoid (Ts-VI) [11], [12]; and Surface Energy Balance (SEB) models [13]. The Surface Energy Balance Algorithm for Land (SEBAL) model was used to estimate ET as a residual of energy balance at the land-air interface. The model described above has gained widespread usage as one of the most effective approaches, requiring minimum ground data and limited knowledge of Earth's surface characteristics [14], [15]. However, it should be noted that being a single-source model, the estimation of evapotranspiration (ET) derived from the Surface Energy Balance Algorithm for Land (SEBA) may be susceptible to errors arising from surface conditions [16]. In a study by Wagle et al. [17], it was observed that surface energy balance models tend to overestimate surface ET under extremely dry conditions. Furthermore, Kiptala et al. [18] demonstrated that the accuracy of ET estimation is significantly affected by crop water stress conditions, primarily due to errors in determining soil heat and sensible heat fluxes.

Thai Binh Plant Protection Department reported that, during the winter rice cultivation in 2015, paddy rice fields were destroyed by blast diseases and insect pests in late March-early April, especially from April 9th to 15th, leading to drying of the infected leaf, and resulting in crop water stress in the eastern districts, including Tien Hai and Thai Thuy districts, and some parts of Kien Xuong District (shown in red color in Figure 1). The paddy rice yield for the Thai Binh Province was 7.163 tonnes per hectare, decreased by 0.09 tonnes per hectare compared with the previous year. It was also reported that the rice grain yield in the eastern districts was relatively lower than in the western districts. Quantitatively speaking, the confirmed disease-infected regions showed lower productivity compared to non-infected areas. The rice yields were 7.16, 7.02, and 7.132 tonnes per hectare in the Thai Thuy, Tien Hai, and Kien Xuong districts, respectively, and 7.24, 7.245, 7.25 tonnes per hectare in the Quynh Phu, Hung Ha, and Dong Hung districts, respectively. The transplantation of year 2015 winter growing season was completed before February 25, while ''reproductive stage'' started before early May, and harvest was done during middle and late May (http://thaibinh.gov.vn/). This study was conducted during ''vegetative stage'' because, in this stage, the morphological and spectral changes of plants can be usually well captured by the optical satellite. In contrast, it is challenging to capture the crop water status during the reproductive stage. The dramatic changes in this phase were caused by the processes of flowering and grain filling that occur under the canopy or inside the hull of rice grains [19].

TABLE 1. Landsat 7 ETM+ bands and geometric resolutions.

Bands	Wavelength (micrometers)	spatial resolution (meters)
Band 1	0.452-0.514	30
Band 2	0.519-0.601	30
Band 3	0.631-0.692	30
Band 4	0.772-0.898	30
Band 5	1.547-1.748	30
Band 6	10.31-12.36	30
Band 7	2.065-2.346	30
Band 8	0.515-0.896	15

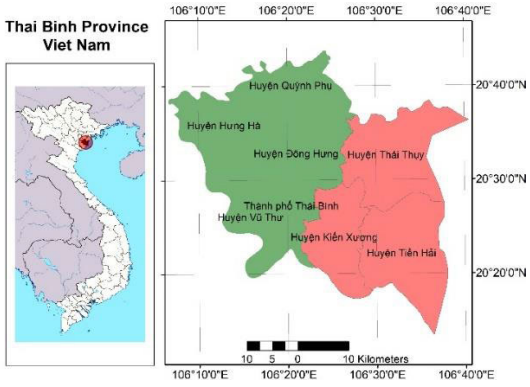

FIGURE 1. Study area, thai binh province, viet nam.

This study aims to further demonstrate the applicability of the recently developed NDLI for providing precise information of plant health conditions. Also, it intends to maximize the potential advantages of NDLI for early detection and quantification of rice plants' response to disease and water shortage conditions by integrating the use of NDLI into thermal infrared portions and surface energy balance theory for assisting the irrigation practice and disease management.

II. METHODOLOGY

This study focuses on the novel approaches for investigating the rice plants' response to water shortage conditions during the growth stage of well-known winter crop cultivated area of Thai Binh Province. The areas affected and unaffected by severe blast diseases and insect pests have been clearly and systematically reported. This is an important prerequisite

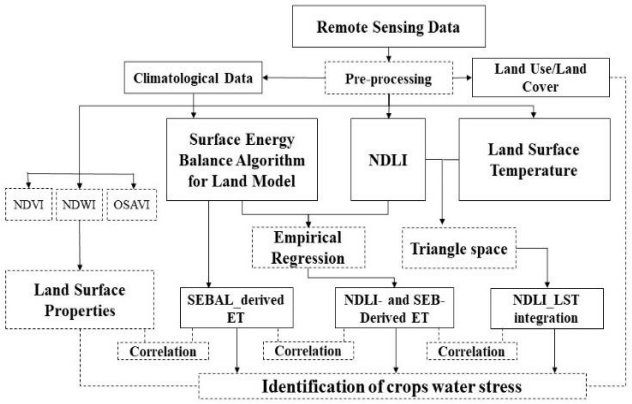

FIGURE 2. Flowchart depicting the major tasks involved in this study.

that contributes to verify the applicability of the experimental study. The Landsat 7 ETM+ images provided by the Landsat program, which is developed by NASA and the United States Geological Survey were used. Landsat 7 ETM+ images consist of eight bands with the spatial resolution of 30 meters for spectral bands and 15 meters for panchromatic band. The approximate scene size of image is 170 km north-south by 183 km east-west.

Figure 2 presents the research flow chart performed in this research. The satellite images were collected from the United States Geological Survey USGS (http://earthexplorer.usgs.gov/) for the primary winter growing season of 2015 over different stages of crop growth, including land preparation (November 20, 2014), growth stage (April 13, 2015), and after harvest (July 02, 2015). Image preprocessing was conducted to remove bad pixels and correct inconsistencies in the data. The area of interest is subsequently extracted from data for further analysis. Ground observations of Thai Binh weather station (20.25°N, 106.23°E), including air temperature (Celsius), air relative humidity (%), and wind speed (m/s), and pressure (hectopascal) were used as input data in the surface energy balance model. Results are evaluated through their incorporation into the existing land surface biophysical property indicators, including NDVI, NDWI, and OSAVI and compared with the rate of water evaporation to the atmosphere as vapour through the rice plant's as the ET derived from the commonly used model (SEBAL). In addition, the performance of the remote sensing-based method for deriving the healthy status of rice plants was cross-examined by the relevant historical information of 2015 winter growing season provided by Thai Binh Plant Protection Department.

- *Study Area*

The Thai Binh Province is selected as our case study area (Figure 1). It is a flat plain formed by Red River system with a total land area of 1,542 square kilometers. As a major rice-growing area of the Red River Delta, the paddy fields comprise the major part of land use with the main practices of rice cultivation of a smallholder farm. Rice is cultivated twice a year with major cultivation seasons in summer (from mid-June to early October) and winter (from mid-December to late May). The weather is influenced by tropical monsoon with total annual rainfall in Thai Binh about 1704 millimeters (mm) and about 85% of the rainfall (1445 mm) received during rainy. The average temperature ranges from 19°C to 32°C [19].

A. CROP WATER SCARCITY ASSESSMENTS

- Normalized Different Latent Heat Index

In our previous study [8], the NDLI, involving red, green, and SWIR bands, has been proven to be a very effective indicator to extract the information of surface water availability as expressed below:

$$NDLI = \frac{\rho_{Green} - \rho_{Red}}{\rho_{Green} + \rho_{Red} + \rho_{SWIR-1}} \quad (1)$$

where ρ_{Green}, ρ_{Red}, and ρ_{SWIR-1} are surface reflectance in the green (0.519-0.601 μm), red (0.631-0.692 μm), and short wavelength infrared 1 (1.547-1.794 μm) bands of Landsat 7 ETM+, respectively.

Through the enhanced contrast between dry and wet surfaces, the NDLI outperforms the other existing indices to access the potential water availability of the land surface. The drier and wetter conditions of land surface are enhanced and correspond to the lower and higher values of NDLI, respectively.

- Land Surface Temperature

The radiative equation-based method was used to calculate the LST by using thermal band data on board of Landsat image. The LST equation can be expressed as

$$LST = \frac{C_1}{\lambda_i \ln(\frac{C_2}{\lambda_i^5(L_\lambda - I_i^{\uparrow} - \tau_i(1-\varepsilon_i)I_i^{\downarrow})/\tau_i\varepsilon_i} + 1)} \quad (2)$$

where C_1 is 14387.7 μm·K;

C_2 is 1.19104×10^8 W·μm^4·m^{-2}·sr^{-1};

L_λ is Top of Atmosphere (TOA) radiance W/(m2 ster μm) ;

λ_i is effective band wavelength for band i;

$I_i^{\uparrow}$ is upwelling path radiance;

$I_i^{\downarrow}$ is downwelling path radiance;

τ_i is atmospheric transmittance for channel i when view zenith angle is θ; and

ε_i is land surface emissivity for channel i.

- Surface Energy Balance Algorithm for Land

The SEBAL model is an iterative process in which the exchange of energy at the land-air interface is balanced through land surface processes such as radiation, convection, conduction, etc., which can be expressed as:

$$\lambda_{ET} = R_n - -G - H \quad (3)$$

where R_n is the net radiation (W m^{-2}), G is the soil heat flux (W m^{-2}), H is the sensible heat flux (W m^{-2}), and λ_{ET} is the instantaneous latent heat flux (W m^{-2}) [20]. Energy exchange at the land-air interface can be properly described

by the energy and mass transport governing equation. The ET (mm/hour) is decided based on the below equation [13], [21], [22]:

$$ET = 3600(\lambda_{ET}/\lambda) \quad (4)$$

where λ is the latent heat of vaporization.

Note that R_n is also known as the actual radiant energy available at the surface [23], [24]. It can be determined as the balance between incoming and outgoing radiations as described below:

$$R_n = R_{s\downarrow}(1-\alpha) + R_{L\downarrow} - R_{L\uparrow} - (1-\varepsilon_0)R_{L\downarrow} \quad (5)$$

where $R_s \downarrow$ and $R_L \downarrow$ are, respectively, the incoming short-wave solar radiation and incoming long-wave radiation reaching the earth's surface (W m^{-2}), α is the surface short-wave albedo (dimensionless), ε_0 is the land surface emissivity (dimensionless), and $R_L \uparrow$ is the outgoing long-wave radiation (W m^{-2}).

Soil heat flux (G) refers to the thermal energy utilized to either warm or cool the volume of soil in the substrate [13]. Generally, G is calculated utilizing the empirical relation function of net radiation and a few other surface parameters [15]:

$$\frac{G}{R_n} = T_s(0.0038 + 0.0074\alpha)(1 - 0.98NDVI^4) \quad (6)$$

where T_s (Celsius) was acquired by thermal infrared sensor using Radiation Transfer Equation method [25].

Sensible heat flux (H) is the exchange of heat caused by the difference in temperature between surface and atmosphere [22]. For H's estimation, two pixels were chosen as two "anchor" samples, which were assumed as the wettest and driest agriculture pixels [22], [26]. The Monin-Obukhov theory was involved in SEBAL as an iterative process for buoyancy effect correction [27])

$$H = \rho_{air} C_p dT \frac{ku*}{\ln(\frac{z_2}{z_1}) - \psi_{h(z_2)} + \psi_{h_{(z_1)}}} \quad (7)$$

where ρ_{air} is the air density (kg m-3), C_p is the specific heat of air at constant pressure (J kg^{-1} K^{-1}), dT is the surface-air temperature difference (Kevin), u* is the local scale friction velocity (m s^{-1}), which is quantified by a function of given observation of wind speed, κ is the von Karman constant, $\psi_{h(z_2)}$ and $\psi_{h(z_1)}$, the stability corrections for heat transport, are computed based on the functions of Paulson [28] and Webb [29], and z_1 and z_2, two near-surface heights of 0.1 m and 2 m, respectively [30].

- Crop water scarcity assessments

In this study, two approaches were adopted for early detection and quantification of plants' response to disease and water shortage conditions. Firstly, the potential advantages of NDLI as the surface water availability indicator was integrated into the indicator of thermal property through triangle space to understand the status of rice canopy and characterize the response of plant water status to the thermal environment.

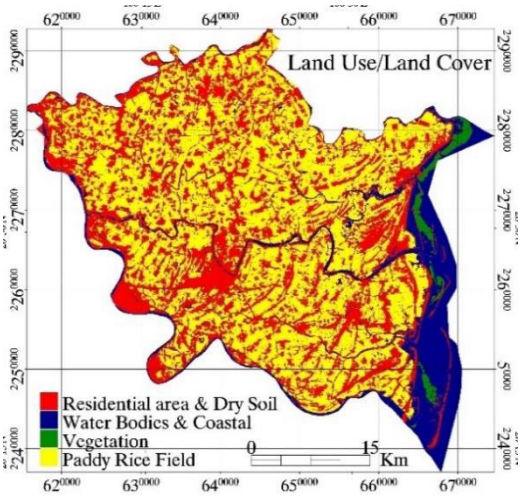

FIGURE 3. Land cover land used.

Secondly, NDLI was integrated into the surface energy balance model to improve the estimation of ET for paddy under unfavourable conditions. An empirical relation is established between NDLI and ET derivatives from the SEBAL over a district that was not affected by pests or diseases during the winter growing season in 2015. A set of independent points randomly chosen from the Dong Hung District were used as training data for the regression model. The land surface features of the selected training area represent the entire study area since the percentage shares of land cover types are 64.9 %, 32.4 %, 2.4%, and 0.3% for paddy rice fields, residential/dry soil, water bodies/coastal lands, and vegetation, respectively. The number of training points was proportional to the appearance frequency of each class. The minimum distance was used to avoid pseudo-replication and increase the generality of the training data. A residual plot was examined for checking the model assumptions. It reveals that a nonlinear regression model, i.e. an asymptotic regression model, can provide a decent fit to the correlation between NDLI and SEBAL-derived ET. The best-fitting model was then applied to create NDLI- and SEB-derived ET for the entire Thai Binh Province. The performance of NDLI-based methods quantified in terms of Percentage Error (PE) and Pearson's correlation coefficient in comparison with reference surface properties indicators and ET, respectively.

B. PADDY RICE MAPPING AND LAND COVER CLASSIFICATION

The distinction of the surface canopy during different stages of crop growth and development significantly affects the accuracy of land cover classification [31], [32], [33]. In this study, time-series Landsat images were employed to overcome single date weakness to classify the paddy field so that multi-date combination images were produced by overlaying different bands of three single-date images (bands 2, 3, 4, 5, and 7) to classify the paddy field. The combination of information obtained from field survey data, high-resolution imagery of the study area from Google Earth taken on April

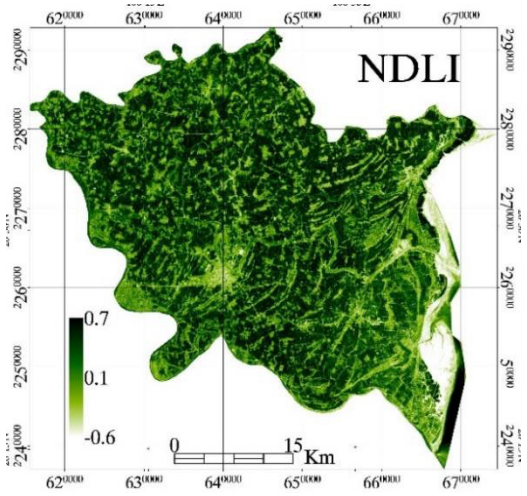

FIGURE 4. Normalized difference latent heat index.

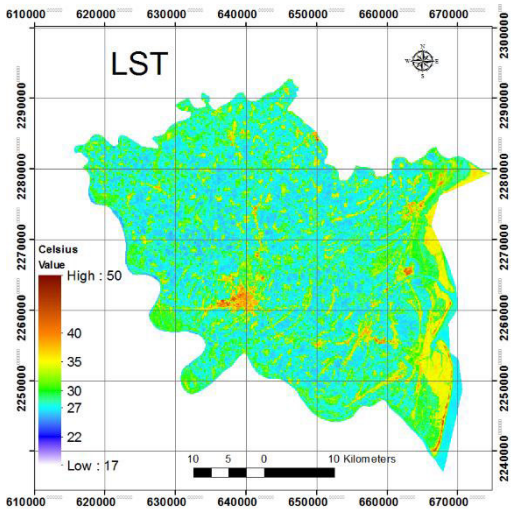

FIGURE 5. Land surface temperature.

13, 2015, and authors' knowledge of rice cultivation and surface spectral reflectance characteristics was used to understand land use and create the decision rules for training sample selection. The maximum likelihood classification method was applied to classify the surface into two categories, including paddy and non-paddy. The non-paddy land covers include water bodies, residential areas, and vegetation. Google Earth Pro was used as a reference for land cover classification validation based on the training data randomly selected within the study area. The fifteen bands combination showed better performance with an overall accuracy of 0.863 compared to single date data with overall accuracies of 0.826 and 0.716 for growth and after harvest stages, respectively. The land cover types in the Thai Binh Province are described in Figure 3. This area is shown as a mix of cropland and rural residential areas. The paddy rice field area detected by the combination image is 869.6 km^2 with a small error (8.6%) as compared to the statistics. Paddy rice agriculture appeared throughout most of the study area except the Thai Binh City and coast where built-up and tide flats dominated the land cover.

III. RESULTS AND DISCUSSION

A. NORMALIZED DIFFERENCE LATENT HEAT INDEX

The NDLI map was derived from the Landsat 7 ETM+ image taken at 10:16 a.m. (local time) on April 13, 2015 (as shown in Figure 4). It is observed that the NDLI well represents the water availability signatures of various land covers. Most NDLI values fall within a range from -0.1 to 0.25 that are correlated with the amount of water contained in land. Higher and lower NDLI values, respectively, correspond to the water bodies and inundated areas, and dry surface, such as dry soil or construction areas. As the vegetation cover contributes to the increase in the value of NDLI, lower and higher NDLI values correspond to the shrub areas and densely vegetated areas (such as crops and dense vegetation areas), respectively. In general, the value of NDLI is strongly linked to the density and condition of the vegetation. Figure 4 shows that the paddy rice areas can be clearly distinguished in the NDLI map with typical values from 0.05 to 0.2. In this stage, since the plant canopy is near 100% coverage over the cropland, the reflectance of crop canopy reaches its peak at the green wavelength region, whereas the strong absorption of pigmentation gives low reflectance at the red wavelength region [34]. However, in order to demonstrate the advantage of NDLI in crop ET estimation and reveal the status of plant water shortage, this study was conducted under non-optimal conditions due to the presence of pests and diseases in some crop field areas, leading to abnormal negative or low NDLI values of rice fields during the active growing period. A high contrast in the values of NDLI is seen in certain regions of the Thai Binh City where the construction lands are surrounded by agriculture areas. Figure 4 indicates that built-up features can be easily distinguished from the other surface types as the negative and positive values of NDLI correspond to built-up/impervious surfaces and agriculture/vegetation lands, respectively. The lowest values of NDLI are observed in the eastern part where tidal flats are characterized by mud and sand. Tidal flats are either covered or uncovered by seawater in different times depending on the tide cycle. The image was taken at 10:30 a.m. (local time) when tidal flats were uncovered at low tide leading to a very low value of NDLI. In contrast, the highest value of NDLI corresponds to the ocean surface in the eastern part of Thai Binh Province.

B. THE NDLI_LST INTEGRATION OVER PADDY RICE FIELD

LST has long been used as an indicator of crop health because of its response to plant moisture content and actual ET [35], [36]. A large quantity of water contained in a material leads to increase in ET and decrease in LST. This study was conducted in the known paddy fields during crop growth stage when canopy reaches its full coverage. In this period, surface reflectance is nearly represented by the status of crop canopy and plant water content is well presented by the transpiration. LST map is derived by leveraging the TM thermal channel of Landsat satellite imagery and presented in Figure 5. The scatter plot (Figure 6) shows a clear trend of decreasing LST

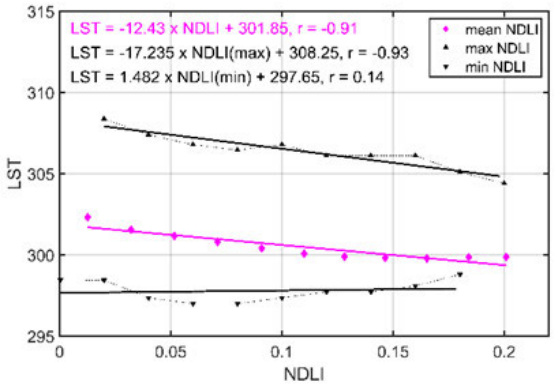

FIGURE 6. Triangle space between NDLI and LST.

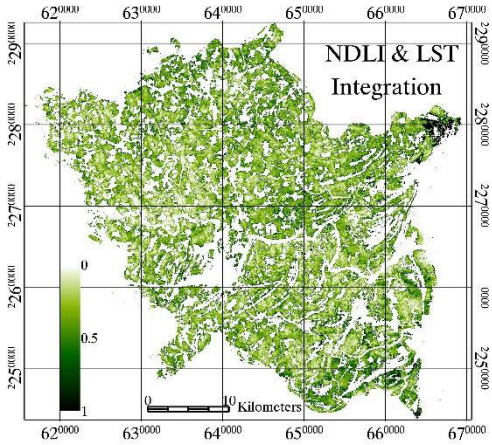

FIGURE 7. Integration between NDLI and LST.

with increasing vegetation water stress, as represented by NDLI. This is in line with the well-established understanding that decreased plant water content often results in a significant increase in canopy temperature.

Figure 7 presents the integration map between NDLI and LST. The figure also illustrates the differences of pixel values correspond to variations in the health conditions of the plants across different areas. The pixe's value ranges from 0 to 1. In general, the value is typically evenly distributed over the entire study area since paddy rice is the predominant crop grown of Thai Binh Province. The results showed that there was a significant change in the pixels value corresponding to the plant health status in the different areas. Lower value appeared in the western part; while higher value was observed over some paddy rice fields in the eastern part of the study area. This is likely due to the existence of rice plants under stress as the decrease of plant water content over the confirmed disease-infected paddy fields in the eastern part of the Thai Binh Province, including Tien Hai and Thai Thuy districts, and some parts of Kien Xuong districts. It is consistent with the fact that amount of water content and canopy temperature are strongly associated as the condition in a plant caused by any agents that interferes with its normal growth and development.

SEBAL-derived ET was used as the reference data to evaluate the performance of integration between NDLI and LST in the providing precise information of plant health conditions. The values of ET calculated from SEBAL model over rice paddies of Thai Binh Province shown in Figure 8 with a unique value for each pixel is average ET of 30 square meters area. The integration between NDLI and LST exhibited its impressive performance in evaluation of plant water content by showing its consistency with potential ET during the reference crop growth stage (correlation coefficient of -0.82) when water release from rice plants becomes a dominant component of ET. Concerning the effect of healthy status of rice plants on land-atmosphere exchanges, the development of plant is associated with the increase of water content in canopy, enhanced canopy transpiration, and thus increased contribution rates to surface ET. The inverse relationship of spatial distributions was shown in Figures 7 and 8, visible indications of plant water stress were observed in the eastern paddy fields of Thai Binh Province, where rice crops were confirmed to be suffering from health problems due to disease infections. On the other hand, the western paddy fields, spanning across Dong Hung, Hung Ha, Kien Xuong, Quynh Phu, and Vu Thu districts, as well as Thai Binh City, showed evenly distributed values with no apparent signs of water stress.

C. NDLI- AND SEB- DERIVED ET OVER PADDY RICE FIELD

Figure 9 presents the NDLI-derived ET in the irrigated rice cultivation area of Thai Binh Province. Results indicate that NDLI- and SEB-derived ET is relatively similar across the paddy rice field with values ranging from 0.45 to 0.75 mm/hour and average ET of 0.65 mm/hour. It is in good accordance with the crop production system. Figure 9 shows the relatively even distribution of ET in the homogeneous paddy rice systems. Results indicate that NDLI- and SEB-derived ET differs from that derived from SEBAL (Figure 10) by less than 10% over 98.1% of the rice fields. These results demonstrate the robust performance of NDLI to obtain the ET of homogeneous rice fields.

In this study, ET estimations were conducted during the serious crop disease-infected period. The water stress of disease-infected paddy fields was exhibited in the NDLI- and SEB-derived ET maps with lower ET compared to non-infected areas. While the average ET of 0.66 mm/hour appeared in the western districts, the pixel's values less than 0.65 mm/hour occupied most of the areas of infected paddy fields in the eastern districts. Figure 9 presents the lower ET value over confirmed disease-infected rice fields in the eastern districts compared to other districts. In contrast, the performance of SEBAL model exhibited that ET appears slightly higher in the confirmed disease-infected rice fields in the eastern districts compared to those found in the northwest Thai Binh Province (as shown in Figure 8). Figure 10 shows the percentage error in ET calculated from the NDLI- and SEB-based methods compared to the ET derived by SEBAL. The NDLI- and SEB-derived ET was found to be lower than the SEBAL-derived ET over the disease-infected rice fields

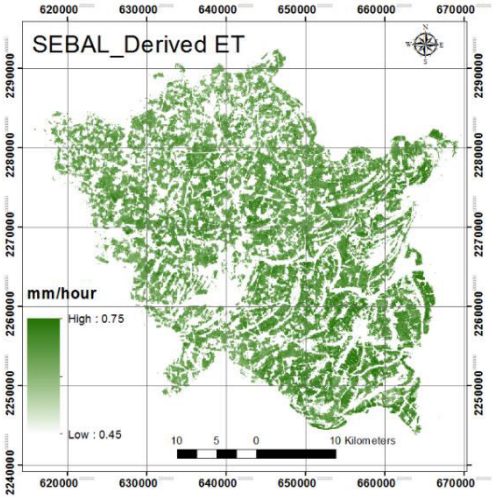

FIGURE 8. SEBAL-derived ET.

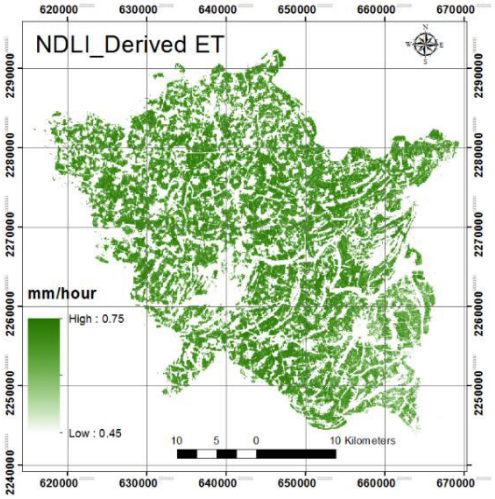

FIGURE 9. NDLI-derived ET.

in the eastern parts of Thai Binh Province, with a percentage error of approximately 10%. Results exhibit high sensibility of NDLI- and SEB-derived ET to the amount of water content in the rice plant. Alternatively, SEBAL-derived ET indicates that a small area in the northeast region of Thai Binh Province represents a notably low ET (less than 0.58 mm/hour) compared to the rice paddies in other areas. However, this area was checked by the determination of crop growing season characteristics. It reveals that plants' health was in a good condition, corresponding to a high rate of ET. The status of rice paddy in this area was presented well in the map of NDLI- and SEB-derived ET, with the values typically higher than 0.65 mm/hour. This rate is around 20% higher than the ET rate calculated using SEBAL (The PE range is shown to be lower than -20% in Figure 10).

Multispectral satellite indices were commonly used to determine crop water status due to their positive correlation with the crop cover fraction, stomatal conductance, and leaf water potential. The investigated indices, derived from Landsat 7 ETM+ taken at 10:16 a.m. (local time) on April 13,

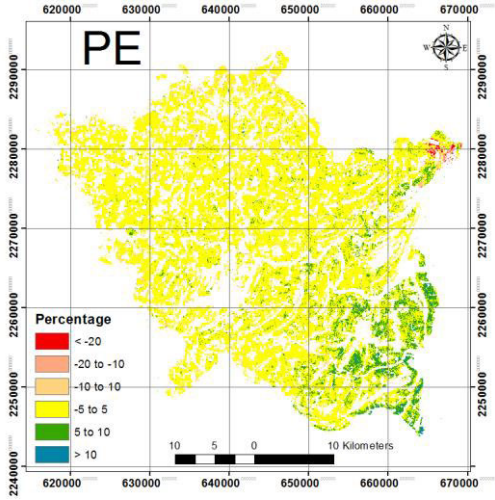

FIGURE 10. Percentage error between NDLI- and SEB- derived ET & SEBAL-derived ET.

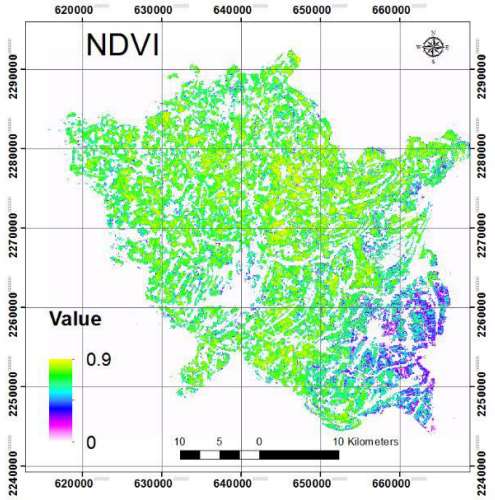

FIGURE 11. Normalized difference vegetation index.

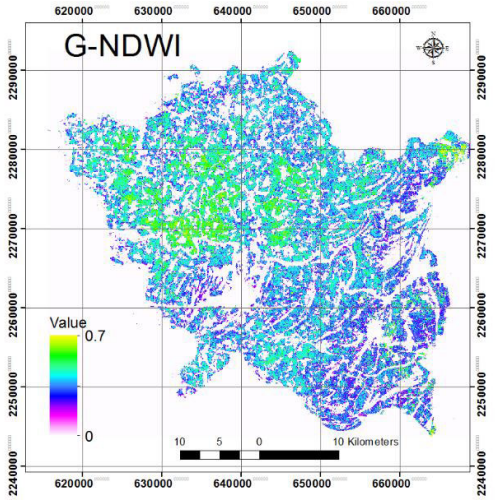

FIGURE 12. Normalized difference water index.

2015, are shown in figures 11, 12, and 13. Results of this study indicate that the spatial pattern of NDLI- and SEB-derived ET

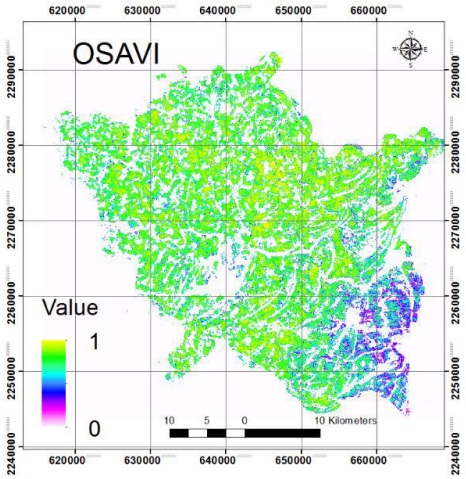

FIGURE 13. Optimised soil adjusted vegetation index.

is generally consistent with spectral water indices across the whole study area. The relationships between NDLI- and SEB-derived ET and investigated indices were assessed against the reference points chosen randomly. The high correlations were found with the positive correlations of 0.84, 0.55, and 0.84 with NDVI, NDWI, and OSAVI, respectively.

The studies and applications of crop irrigation are primarily based on the crop water requirement. The ET investigation may deviate due to non-optimal conditions, such as the presence of pests and diseases, water shortage, or waterlogging. NDLI has been proven to be an effective indicator for reliable estimation of ET and rapid assessment of crop water status since NDLI can be easily implemented without requiring any preliminary knowledge of the soil line parameters. NDLI- and SEB-derived ET reflects the field conditions of the rice plant to reveal several important aspects regarding crop growth, suggesting its sensitivity to the impairment of rice plant normal state and rough amount of required water. Thus, it could be used as a reference for taking quick and suitable measures to optimize the efficiency of agricultural production and irrigation management. Furthermore, time-series crop ET estimation that is reflected by the temporal fluctuation of NDLI is a great potential approach for further agronomical researches.

IV. CONCLUSION

This study aims to utilize multi-spectral remote sensing data to enhance the efficacy of NDLI, as previously demonstrated in our work. The objective is to improve the accurate analysis of crop plant conditions and provide reliable information regarding water scarcity in rice-growing areas. The results exhibit the impressive performance of NDLI-based methods in determination of plant-health status and evaluation of plant-water content. NDLI-based methods show its consistency with the indicators of crop plants properties and evapotranspiration. Also, the NDLI-based methods proved their capacity to identify water stress of rice plants under non-optimal conditions, such as the impacts of diseases, water shortage.

The NDLI- and SEB-derived ET is a potential indicator for revealing the abnormal growth and/or impairment of crop plant. NDLI- and SEB-derived ET was found to represent well the water shortage status over the confirmed disease-infected rice fields that cannot be well detected by SEBAL. Such improvement is crucial to support the decision makers to properly utilize the water resources for irrigation management, especially under the circumstance of relatively dry environment. Besides, the NDLI- and SEB-derived ET shows a high-degree consistency with SEBAL-derived ET with difference less than 10% for over 98.1% rice paddy field of the study site in the Thai Binh Province.

The exhibited characteristics of the NDLI bring potential benefits to a wide variety of studies or practices related to crop water status. These benefits may be further explored and examined in the future studies since NDLI's formula is very simple and may be easily implemented. Also, the use of NDLI to derive ET over a longer term during the growing season is of interest to further develop means to improve the seasonal water use of paddy rice or other crop types. It is important to address the possible shortage of this paper related to the presentation of data constrained by a single-day case. Inclusion of data from the other dates would significantly increase the robustness of the study since there is a need to conquer the difficulty to obtain the field data for further studies.

ACKNOWLEDGMENT

Satellite data are supported by United States Geological Survey (USGS).

REFERENCES

[1] D. I. Guest, "Plant pathology, principles," in *Encyclopedia of Applied Plant Sciences*, 2nd ed., B. Thomas, B. G. Murray, and D. J. Murphy, Eds. Oxford, U.K.: Academic, 2017, pp. 129–136.

[2] T. Gayathri Devi and P. Neelamegam, "Image processing based rice plant leaves diseases in Thanjavur, Tamilnadu," *Cluster Comput.*, vol. 22, no. S6, pp. 13415–13428, Nov. 2019.

[3] J. Keeley and J. H. Lehr, *Water Encyclopedia, Surface and Agricultural Water*. Hoboken, NJ, USA: Wiley, 2005.

[4] W. G. M. Bastiaanssen, D. J. Molden, and I. W. Makin, "Remote sensing for irrigated agriculture: Examples from research and possible applications," *Agricult. Water Manage.*, vol. 46, no. 2, pp. 137–155, Dec. 2000.

[5] C. J. Tucker and B. J. Choudhury, "Satellite remote sensing of drought conditions," *Remote Sens. Environ.*, vol. 23, no. 2, pp. 243–251, 1987, doi: 10.1016/0034-4257(87)90040-X.

[6] S. K. McFeeters, "The use of the normalized difference water index (NDWI) in the delineation of open water features," *Int. J. Remote Sens.*, vol. 17, no. 7, pp. 1425–1432, May 1996.

[7] G. Rondeaux, M. Steven, and F. Baret, "Optimization of soil-adjusted vegetation indices," *Remote Sens. Environ.*, vol. 55, no. 2, pp. 95–107, Feb. 1996.

[8] Y. Liou, M. S. Le, and H. Chien, "Normalized difference latent heat index for remote sensing of land surface energy fluxes," *IEEE Trans. Geosci. Remote Sens.*, vol. 57, no. 3, pp. 1423–1433, Mar. 2019, doi: 10.1109/TGRS.2018.2866555.

[9] R. D. Jackson, R. J. Reginato, and S. B. Idso, "Wheat canopy temperature: A practical tool for evaluating water requirements," *Water Resour. Res.*, vol. 13, no. 3, pp. 651–656, Jun. 1977.

[10] C. Huang, Y. Li, J. Gu, L. Lu, and X. Li, "Improving estimation of evapotranspiration under water-limited conditions based on SEBS and MODIS data in arid regions," *Remote Sens.*, vol. 7, no. 12, pp. 16795–16814, Dec. 2015.

[11] R. Tang, Z.-L. Li, and B. Tang, "An application of the Ts–VI triangle method with enhanced edges determination for evapotranspiration estimation from MODIS data in arid and semi-arid regions: Implementation and validation," *Remote Sens. Environ.*, vol. 114, no. 3, pp. 540–551, Mar. 2010.
[12] L. Jiang and S. Islam, "A methodology for estimation of surface evapotranspiration over large areas using remote sensing observations," *Geophys. Res. Lett.*, vol. 26, no. 17, pp. 2773–2776, Sep. 1999.
[13] Z. L. Li et al., "A review of current methodologies for regional evapotranspiration estimation from remotely sensed data," *Sensors*, vol. 9, no. 5, pp. 53–3801, May 2009, doi: 10.3390/s90503801.
[14] M. Mkhwanazi, J. Chávez, and A. Andales, "SEBAL—A: A remote sensing ET algorithm that accounts for advection with limited data. Part I: Development and validation," *Remote Sens.*, vol. 7, no. 11, pp. 15046–15067, Nov. 2015.
[15] Z. Sun, B. Wei, W. Su, W. Shen, C. Wang, D. You, and Z. Liu, "Evapotranspiration estimation based on the SEBAL model in the Nansi lake wetland of China," *Math. Comput. Model.*, vol. 54, nos. 3–4, pp. 1086–1092, Aug. 2011.
[16] A. L. Ruhoff, A. R. Paz, W. Collischonn, L. E. O. C. Aragao, H. R. Rocha, and Y. S. Malhi, "A MODIS-based energy balance to estimate evapotranspiration for clear-sky days in Brazilian tropical savannas," *Remote Sens.*, vol. 4, no. 3, pp. 703–725, Mar. 2012.
[17] P. Wagle, N. Bhattarai, P. H. Gowda, and V. G. Kakani, "Performance of five surface energy balance models for estimating daily evapotranspiration in high biomass sorghum," *ISPRS J. Photogramm. Remote Sens.*, vol. 128, pp. 192–203, Jun. 2017.
[18] J. K. Kiptala, Y. Mohamed, M. L. Mul, and P. Van der Zaag, "Mapping evapotranspiration trends using MODIS and SEBAL model in a data scarce and heterogeneous landscape in eastern Africa," *Water Resour. Res.*, vol. 49, no. 12, pp. 8495–8510, Dec. 2013.
[19] K. Guan, Z. Li, and L. N. Rao, "Measuring rice yield from space: The case of Thai Binh Province, Vietnam," Asian Develop. Bank Econ., Mandaluyong, Philippines, Working Paper Series no. 541, 2018.
[20] D. Autovino, M. Minacapilli, and G. Provenzano, "Modelling bulk surface resistance by MODIS data and assessment of MOD16A2 evapotranspiration product in an irrigation district of Southern Italy," *Agricult. Water Manage.*, vol. 167, pp. 86–94, Mar. 2016.
[21] W. G. M. Bastiaanssen, "SEBAL-based sensible and latent heat fluxes in the irrigated Gediz basin, Turkey," *J. Hydrol.*, vol. 229, nos. 1–2, pp. 87–100, Mar. 2000.
[22] R. Allen, M. Tasumi, R. Trezza, R. Waters, and W. Bastiaanssen, "Surface energy balance algorithm for land (SEBAL)–Advanced training and users manual, Idaho implementation," Idaho Dept. Water Resour., NASA EOSDIS, Raytheon Company, version 1.0, 2002.
[23] Y.-A. Liou and S. Kar, "Evapotranspiration estimation with remote sensing and various surface energy balance algorithms—A review," *Energies*, vol. 7, no. 5, pp. 2821–2849, Apr. 2014.
[24] Y.-A. Liou, J. F. Galantowicz, and A. W. England, "A land surface process/radiobrightness model with coupled heat and moisture transport for Prairie grassland," *IEEE Trans. Geosci. Remote Sens.*, vol. 37, no. 4, pp. 1848–1859, Jul. 1999.
[25] X. Yu, X. Guo, and Z. Wu, "Land surface temperature retrieval from Landsat 8 TIRS—Comparison between radiative transfer equation-based method, split window algorithm and single channel method," *Remote Sens.*, vol. 6, no. 10, pp. 9829–9852, Oct. 2014.
[26] T.-T. Shi, D.-X. Guan, J.-B. Wu, A.-Z. Wang, C.-J. Jin, and S.-J. Han, "Comparison of methods for estimating evapotranspiration rate of dry forest canopy: Eddy covariance, Bowen ratio energy balance, and penman-monteith equation," *J. Geophys. Res.*, vol. 113, no. D19, 2008.
[27] G. Paul, P. H. Gowda, P. V. Prasad, T. A. Howell, S. A. Staggenborg, and C. M. U. Neale, "Lysimetric evaluation of SEBAL using high resolution airborne imagery from BEAREX08," *Adv. Water Resour.*, vol. 59, pp. 157–168, Sep. 2013.
[28] C. A. Paulson, "The mathematical representation of wind speed and temperature profiles in the unstable atmospheric surface layer," *J. Appl. Meteorol.*, vol. 9, no. 6, pp. 857–861, Dec. 1970.
[29] E. K. Webb, "Profile relationships: The log-linear range, and extension to strong stability," *Quart. J. Roy. Meteorological Soc.*, vol. 96, no. 407, pp. 67–90, Jan. 1970, doi: 10.1002/qj.49709640708.
[30] W. G. M. Bastiaanssen, E. J. M. Noordman, H. Pelgrum, G. Davids, B. P. Thoreson, and R. G. Allen, "SEBAL model with remotely sensed data to improve water-resources management under actual field conditions," *J. Irrigation Drainage Eng.*, vol. 131, no. 1, pp. 85–93, Feb. 2005.
[31] P. Dao and Y.-A. Liou, "Object-based flood mapping and affected rice field estimation with Landsat 8 OLI and MODIS data," *Remote Sens.*, vol. 7, no. 5, pp. 5077–5097, Apr. 2015.
[32] Y.-A. Liou et al., "Assessment of disaster losses in rice paddy field and yield after Tsunami induced by the 2011 great east Japan earthquake," *J. Mar. Sci. Technol.*, vol. 20, no. 6, pp. 618–623, 2012, doi: 10.6119/jmst-012-0328-2.
[33] M. Traore, M. S. Lee, A. Rasul, and A. Balew, "Assessment of land use/land cover changes and their impacts on land surface temperature in Bangui (the capital of central African republic)," *Environ. Challenges*, vol. 4, Aug. 2021, Art. no. 100114.
[34] E. B. Knipling, "Physical and physiological basis for the reflectance of visible and near-infrared radiation from vegetation," *Remote Sens. Environ.*, vol. 1, no. 3, pp. 155–159, Jun. 1970.
[35] D. Sun and R. T. Pinker, "Case study of soil moisture effect on Land Surface Temperature retrieval," *IEEE Geosci. Remote Sens. Lett.*, vol. 1, no. 2, pp. 127–130, Apr. 2004.
[36] M. Pablos, M. Piles, N. Sánchez, V. González-Gambau, M. Vall-llossera, A. Camps, and J. Martínez-Fernández, "A sensitivity study of land surface temperature to soil moisture using in-situ and spaceborne observations," in *Proc. IEEE Geosci. Remote Sens. Symp.*, Jul. 2014, pp. 3267–3269.

MAI SON LE received the B.S. degree from the Faculty of Environmental Science, Hanoi University of Science, Vietnam National University, Vietnam, in 2011, the M.S. degree from the Space and Application Department, University of Science and Technology of Hanoi, Vietnam, in 2014, and the Ph.D. degree from the Graduate Institute of Hydrological and Oceanic Sciences, National Central University, Taiwan, in 2021. He is currently pursuing the Ph.D. degree with the Space Technology Institute, Vietnam. Since 2011, he has been a Research Assistant with the Vietnam Academia of Science and Technology, Vietnam. His research interests include surface energy balance, hydrology, spatial analysis, and remote sensing.

YUEI-AN LIOU (Senior Member, IEEE) received the B.S. degree in electrical engineering from National Sun Yat-sen University, Taiwan, in 1987, and the M.S.E. degree in electrical engineering (EE), the M.S. degree in atmospheric and space sciences, and the double Ph.D. degree in EE and atmospheric, oceanic, and space sciences from the University of Michigan, Ann Arbor, USA, in 1992, 1994, and 1996, respectively. He is currently the Honorary President of the Taiwan Group on Earth Observations, the Honorary President of the Vietnamese Experts Association in Taiwan, and a Distinguished Professor with the Center for Space and Remote Sensing Research, National Central University. His current research interests include GPS meteorology and ionosphere, remote sensing of the atmosphere, land surface, and polar ice, and land surface processes modeling. He is a Foreign Member of the Russian Academy of Engineering Sciences and a member of the International Academy of Astronautics. He serves as an editor for several prestigious journals and published more than 200 referral papers with H-Index 43.

MINH TUAN PHAM received the B.S. degree in information technology from the Hanoi University of Science and Technology, Vietnam, in 1997, and the M.S. and Ph.D. degrees in control engineering from Nanyang Technological University, Singapore, in 2002 and 2006, respectively. He is currently the Vice Director of the Space Technology Institute, Vietnam Academia of Science and Technology, Vietnam.